Gas Flow Dynamics in Hollow-Fiber Membranes

William J. Federspiel
Artificial Lung Program, Dept. of Surgery, Dept. of Chemical Engineering, and Bioengineering Program

Jeffrey L. Williams
Bioengineering Program

Brack G. Hattler
Artificial Lung Program, Dept. of Surgery

University of Pittsburgh, Pittsburgh, PA 15219

Biomedical and chemical separations often use hollow-fiber membranes for exchanging diffusible species between segregated gas and liquid flow streams. A classic example is the hollow fibers used in extracorporeal and intracorporeal artificial lungs (cf., High et al., 1993). In artificial lung devices, oxygen and carbon dioxide diffuse oppositely across the fiber membranes between a blood phase flowing outside the fibers, and a gas phase flowing through the fiber lumen (sweep gas). The principal determinants of exchange are the overall mass-transfer coefficient of the device, the total membrane surface area, and the differences in gas species partial pressure driving the exchange. Although most of the mass-transfer resistance resides within the membrane and blood phases (Qi and Cussler, 1985a,b), the flow dynamics of the sweep gas play a key role by dictating the partial pressure of the exchanging species within the gas phase. That is, for a given species exchange rate (O_2 or CO_2), the fractional gas species concentration along the fiber depends on the sweep gas-flow rate through the fiber, and in turn the species partial pressure along the fiber lumen, the key intrafiber determinant of exchange, depends directly on both the fractional species concentration and the total gas pressure along the fiber. Thus, understanding the gas-flow dynamics (pressure-flow behavior) within hollow-fiber bundles becomes essential to designing oxygenators and to modeling their gas-exchange performance.

The dynamics of gas flow within hollow-fiber membranes may appear superficially as an application of simple incompressible Poiseuille flow theory. The internal caliber of these fibers is generally 300 μm or smaller, and their length to diameter ratios are typically large. For the gas-flow rates usually involved, Reynolds numbers are therefore unity or smaller, and the flow can be considered fully developed and laminar. The incompressible Poiseuille flow paradigm predicts, for example, a linear relation between pressure drop and resulting gas-flow rate (Gerhart et al., 1992). Although the usual indices suggesting compressible flow are small (e.g., Mach number and kinetic energy variations), the gas flow in hollow-fiber membranes cannot necessarily be considered incompressible. The small size of the fibers, coupled with their great relative length, means that flow resistance and pressured drops can be appreciable, and that variations in fluid density are potentially important.

Our interest in studying the gas flow dynamics within hollow-fiber membranes arose as part of development work (Hattler et al., 1992) on an intravenous membrane oxygenator (IMO). All artificial lung devices must flow sufficient O_2 sweep gas to minimize CO_2 accumulation in the fibers, and to avoid reducing CO_2 exchange as a result (cf., High et al., 1993). Extracorporeal oxygenators typically use several thousand fibers in parallel ($\sim$ 4,000 to 8,000), each of a relatively short length ($\sim$ 15 cm or less) and large internal diameter ($\sim$ 250–300 μm). The requisite sweep gas-flow rate ($\sim$ 5 to 15 L/min) for adequate CO_2 exchange therefore engenders a relatively small pressure drop ($< \sim$ 50 mm Hg), and gas compressibility is not important. Conversely, to be insertable in the vena cava without unduly restricting blood flow, an intravenous oxygenator possesses fewer fibers ($\sim$ 1,000) of smaller diameter ($\sim$ 200–250 μm), with longer lengths ($\sim$ 50–60 cm) to provide adequate exchange area (Mortensen and Berry, 1989). The resulting gas-phase flow resistance of an intravenous oxygenator can easily be 50 to 100 times greater than that for extracorporeal oxygenators. Thus the vacuum pressures required in intravenous oxygenators for driving sufficient O_2 sweep gas flow can be several hundred mm Hg. Similarly, intrathoracic artificial lungs also have design constraints which can lead to increased gas-flow resistance and larger vacuum pressure requirements for sufficient sweep gas flow (Fazzalari et al., 1994). Thus, gas compressibility is potentially of much greater importance in the gas-flow dynamics of intracorporeal oxygenators than their extracorporeal counterparts.

Correspondence concerning this article should be addressed to W. J. Federspiel.

This article describes experimental studies of the pressure flow relationship for gas flow through hollow-fiber membranes, and through a prototype IMO. The relevant theory for compressible Poiseuille flow is straightforward, but is surprisingly not easily found in compressible flow treatises. The principal result can be found in the classical treatise of Shapiro (1953), and as a component of a mathematical model of gas permeation through blind-ended glass membranes (Shelekhin et al., 1992). A simple derivation of compressible Poiseuille flow theory is given below for completeness. Experiments were designed using air and helium gases to establish the applicability of the compressible Poiseuille flow paradigm to gas flow through hollow fiber membranes, and to use the theory to evaluate the measured gas-flow dynamics in the IMO prototype. Although the application here is to intracorporeal oxygenation, the results described may have significance to other separation processes involving gas flow through hollow-fiber membranes.

Compressible Poiseuille Flow

Simple estimates can be used to establish the expected gas-flow regime in hollow-fiber membranes under relevant conditions to intravenous oxygenation. The required gas-flow rate through intravenous oxygenators is typically about 5 L/min. Assuming a hollow fiber bundle consisting of 1,000 fibers of $d = 200$ μm, the intrafiber Reynolds number (Re) is less than 50 for air or O_2 flow. The flow is therefore not only laminar, but can be considered fully developed as well because the required normalized entrance length (Gerhart et al., 1992) $Le/d = 0.065\ Re < 3$ is a very small fraction of normalized fiber length $L/d > 1{,}000$. The relevant theory for fully developed compressible viscous flow in a tube follows below.

Consider a single cylindrical fiber of length L and constant cross-sectional area A with (absolute) gas pressures P_o and P_l, imposed across the fiber length. The resulting gas volumetric flow rate $Q(z)$ varies axially (z) along the fiber due to variations in gas density, $\rho(z)$, in the presence of the pressure variation $P(z)$. A momentum balance on a differential length of fiber dz requires that momentum changes across the element balance pressure and viscous forces

$$\frac{\beta}{A^2}\rho Q\frac{dQ}{dz} = \frac{dP}{dz} + \frac{R}{L}Q \tag{1}$$

where β is a velocity profile correction factor for momentum flux, and R is the Poiseuille flow resistance, given by $R = 128\ \mu L/\pi d^4$ for fully developed flow in a tube, with μ the fluid viscosity. Because of the small caliber and relatively long length of a fiber, fluid momentum changes along the fiber are about 100 times smaller than viscous forces. Accordingly, the momentum balance simplifies to

$$\frac{dP}{dz} = -\frac{R}{L}Q \tag{2}$$

The volumetric flow rate $Q(z)$ varies with z in an unknown manner, and so Eq. 2 cannot be integrated directly as for incompressible Poiseuille flow. Nevertheless, the mass-flow rate, $\dot{m} = \rho(z)Q(z)$, is essentially constant along the fiber because in typical application the net mass flux across the fiber wall is negligible compared to mass-flow rate along the fiber. Multiplying Eq. 2 by ρ, introducing the perfect gas relation $P = \rho\,\mathcal{R}T$, and integrating over the length of the tube under isothermal conditions, yields the compressible Poiseuille flow relation. (An energy balance can be used to show that kinetic energy changes are small and flow through the fibers remains essentially isothermal.)

$$P_o^2 - P_l^2 = 2R\,\mathcal{R}T\dot{m} \tag{3}$$

Thus, incorporating gas compressibility into Poiseuille flow gives rise to a nonlinear relationship between pressure drop and mass-flow rate.

Experimental Methods

The pressure flow behavior in hollow-fiber bundles was experimentally investigated using the apparatus illustrated in Figure 1a. The principal components are a regulated compressor as a vacuum source, a mercury manometer, a mass-flow meter (Top-Trak 821-1, Sierra Instruments, Inc., Monterey, CA), and the test hollow fiber bundles. Two different hollow fiber bundles were studied, as illustrated in Figure 1b: a test fiber bank (TFB) of parallel fixed fibers, and an IMO under development in our lab. The TFB was constructed specifically to examine pressure flow behavior within the hollow fibers themselves, and has inlets/outlets opening directly to relatively wide manifolds for distributing and collecting flow from the individual fibers with minimal additional pressure drop. (The estimated dynamic head within the inlet/outlet of the TFB was much less than 1 mm Hg for air and 0.1 mm Hg for helium under conditions of interest.) Conversely, the gas pathway within the IMO device (pre- and postfibers) is more complicated. Gas enters the IMO through a long central conduit and travels distally to a feed manifold where it distributes to the individual hollow fibers. The flow through the fibers collects in an exhaust manifold, then exits the IMO device in an annular outlet pathway leading to the gas outflow port. The TFB and IMO fiber bundles both were composed of Mitsubishi composite hollow fiber membranes (MHF-200L, Mitsubishi Corp., Japan), with an inner diameter of $d = 207$ μm. (The Mitsubishi composite fiber uses a one micron nonporous polyurethane layer within its microporous wall, and so gas flow (permeation) through fiber wall is negligible.) The TFB uses 93 fibers each of 11.5 cm in length, while the IMO bundle consists of 960 fibers of 34 cm length.

One implication of the compressible Poiseuille flow theory (Eq. 3) is that the pressure drop ($P_o - P_l$) for a given mass-flow rate differs for vacuum driven flow ($P_o = P_{atm}$, $P_l < P_o$) compared to positive pressure driven flow ($P_o > P_l$, $P_l = P_{atm}$). As oxygenators typically drive gas flow under vacuum, the regulated compressor was operated to provide a constant vacuum source in the range up to -450 mm Hg gauge. Vacuum driven air flow and helium flow were studied in both the TFB and IMO fiber bundles. For vacuum driven helium flow, a tee, open to the atmosphere as shown in Figure 1a, was placed between the helium supply tank and the fiber bundle, and tank flow was increased until flow out of the tee was evident, thus ensuring that only helium entered the fiber bundles. The fiber bundles were tested in air and also submersed in water. No differences were found in the measured

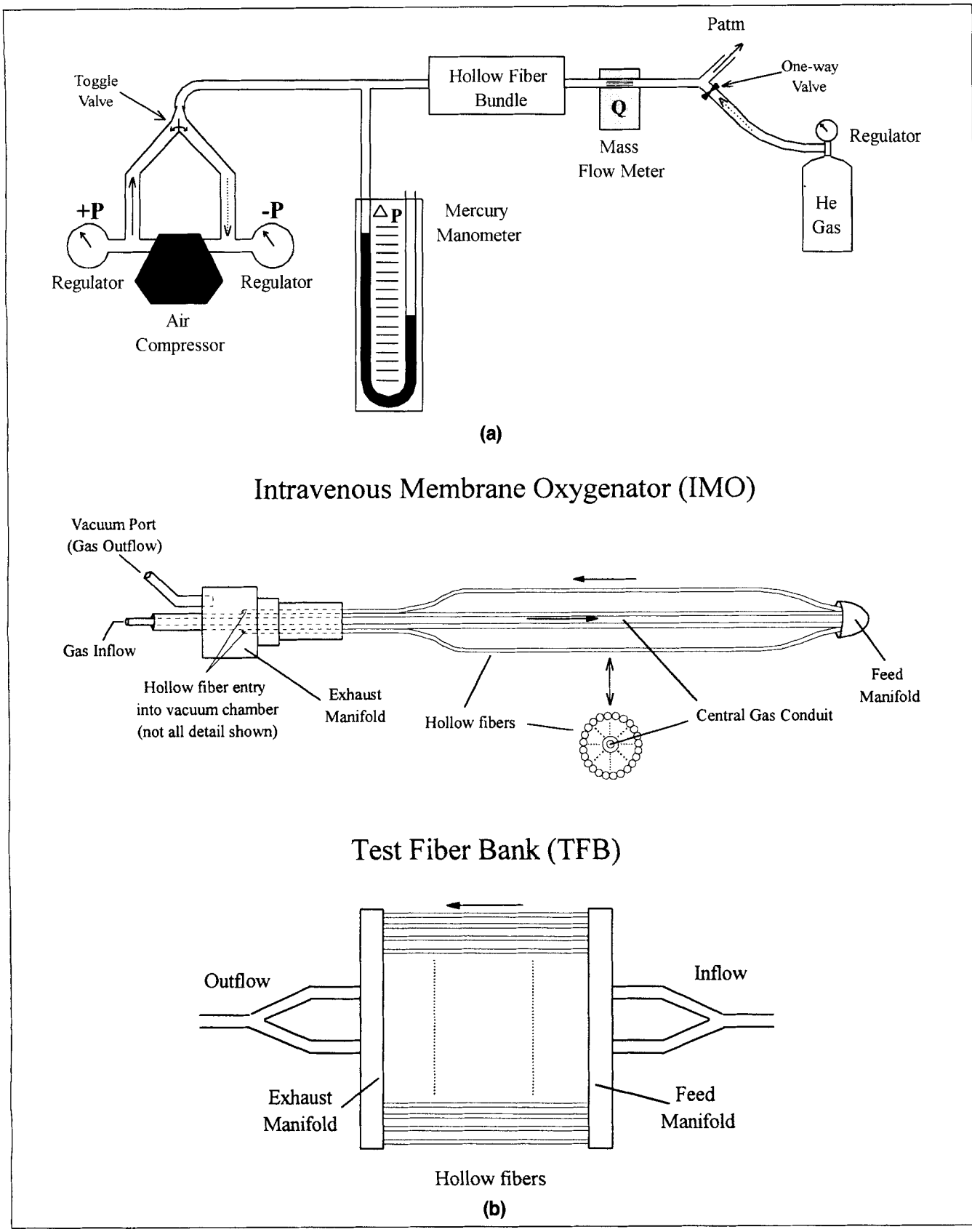

Figure 1. a) Apparatus for measuring pressure and flow in hollow-fiber bundles; b) hollow-fiber bundles: IMO being developed and TFB.

Relation of fibers to device not drawn to scale.

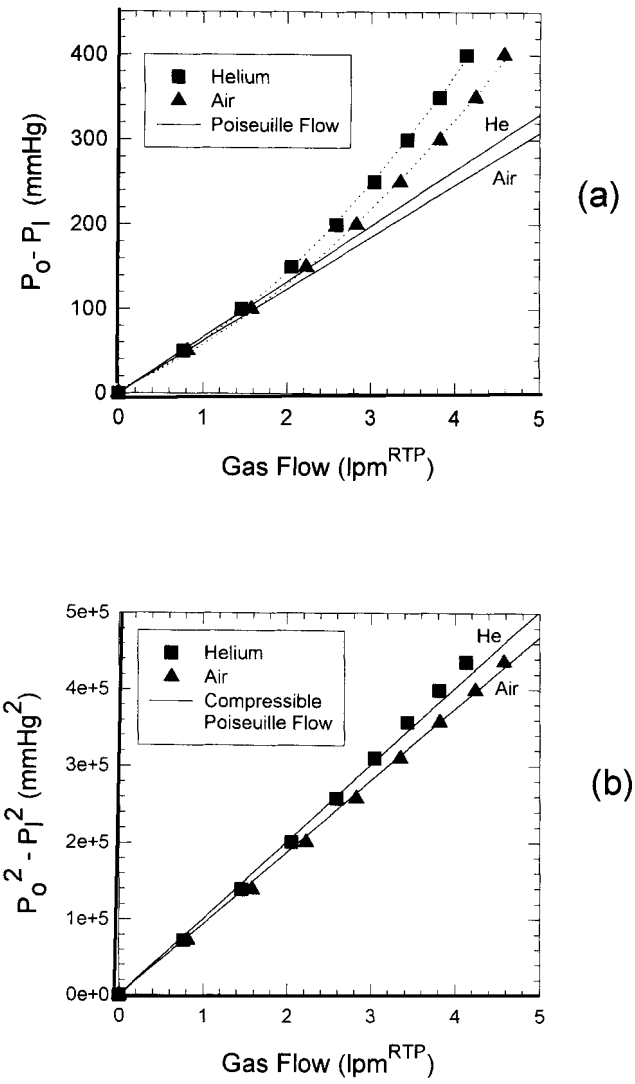

Figure 2. Pressure drop vs. mass-flow rate measured in the TFB for air (▲) and helium (■) flow driven by vacuum pressure: a) incompressible and b) compressible Poiseuille flow form.

The solid lines represent the respective theoretical predictions for these flow paradigms.

pressure flow behavior, indicating that gas permeation in/out of the fiber wall is not significant, due to the composite membrane used.

Pressure-Flow within Hollow Fibers

The principal evidence that gas compressibility affects the flow dynamics within hollow fibers is shown in Figure 2a. Here, the relationship between pressure drop and mass-flow rate measured in the TFB is shown for the flow of helium (■) and air (▲). The mass-flow rate measured by the flowmeter is expressed as a volumetric flow rate in L/min (lpm^{RTP}) at a *reference temperature and pressure* (RTP: T = 25°C and P_{atm} = 760 mm Hg). The solid lines show the predicted pressure flow behavior based on incompressible Poiseuille flow theory $P_o - P_l = RQ$, where R is the Poiseuille flow resistance of the fiber *bank* for either air or helium flow. The experimental pressure flow relationship for both gases deviate consistently from incompressible Poiseuille flow theory above a pressure drop of 100 mm Hg. The deviation cannot be attributed to inertially related pressure drops because helium and air deviate from theory similarly, despite their ten-fold difference in gas density. Furthermore, the pressure drop for helium exceeds that for air, consistent with the greater viscosity for helium than for air ($\mu_{He} = 1.95 \times 10^{-4}$ Poise vs. $\mu_{air} = 1.82 \times 10^{-4}$ Poise).

The application of compressible Poiseuille flow theory to the same experimental pressure-flow behavior is evaluated in Figure 2b. Here, the pressure-flow relations shown in Figure 2a are recast according to the pressure *squared* drop across the fibers ΔP^2 which according to compressible Poiseuille flow theory should vary linearly with mass-flow rate. The solid lines represent compressible Poiseuille flow theory for helium and air with mass-flow rate expressed as a volumetric flow rate Q^{RTP} at RTP. In these terms, mass-flow rate for a perfect gas is

$$\dot{m} = \rho^{RTP} Q^{RTP} = (P_{atm}/\Re T) Q^{RTP} \tag{4}$$

and the compressible Poiseuille relation (Eq. 3) becomes

$$P_o^2 - P_l^2 = 2RP_{atm} Q^{RTP} \tag{5}$$

for flow at the reference temperature. Figure 2b indicates that for both air and helium flow, the compressible Poiseuille flow result (Eq. 5) predicts well the pressure-flow behavior in the hollow fiber test bank over a broad range of pressure drops (0–400 mm Hg). For smaller pressure drops below about 100 mm Hg, the pressure flow relationship can be satisfactorily predicted by incompressible Poiseuille flow theory (Figure 2a).

The experimental data do suggest a small deviation from compressible Poiseuille flow, as evident by some curvilinearity in Figure 2b. That distensibility of the polymer fibers may be responsible for the minor deviation was eliminated by altering the ambient pressure on the outside of the fibers (up to −200 mm Hg) and demonstrating that pressure flow relationships were unaffected. Thus, differences in transmural pressure do not affect flow resistance, and the fibers are essentially rigid tubes. The small deviation from compressible Poiseuille flow also cannot be attributed to departures from assumed isothermal flow. In the limiting nonisothermal case of adiabatic compressibility, the pressure density relation is given by $P = k\rho^{\gamma}$ for a perfect gas, where k is a constant and γ is the specific heat ratio, approximately 1.4–1.6 for air and helium (Kyle, 1984). If this were the case, the compressible Poiseuille flow relation (Eq. 3 or 5) would exhibit a weaker pressure dependence of $\Delta P^{1.6-1.7}$, rather than the ΔP^2 for isothermal compressibility. Furthermore, the temperature decrease associated with nonisothermal expansion would reduce gas viscosity and Poiseuille flow resistance and further reduce the pressure dependence in the compressible Poiseuille flow relation. In contrast, a nonlinear regression to the experimental data for air and helium indicate that a pressure dependence of about $\Delta P^{2.3-2.4}$ would give the least deviation from a linear variation with mass-flow rate.

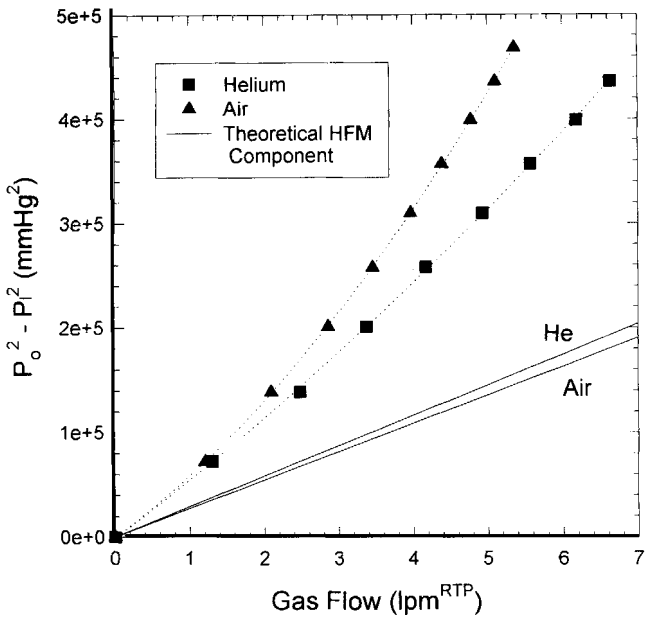

Figure 3. Pressure drop vs. mass-flow rate measured in the IMO for air (▲) and helium (■) flow driven by vacuum pressure.

Results are expressed in the compressible Poiseuille flow form, and the solid lines represent the compressible Poiseuille flow predictions for the assumed fiber bank within the IMO.

Pressure-Flow within the Intravenous Oxygenator

The pressure flow behavior for the IMO is displayed in Figure 3 (in compressible Poiseuille form) for helium (■) and air (▲) flow. The solid lines are the pressure-flow predictions for compressible Poiseuille flow through the hollow fibers of the IMO device. Figure 3 indicates that the pressure drop required for a given air or helium flow rate through the IMO device is substantially larger than can be theoretically attributed to compressible Poiseuille flow through the fiber bundle itself. Thus, either some aspect of flow through the IMO fiber bundle is not well understood, or substantial pressure drops exist in other parts of the IMO gas flow pathway. The discrepancy, however, is not due to an inability to predict pressure-flow behavior within hollow fiber membranes, since the test bank pressure-flow behavior is predicted well by compressible Poiseuille flow theory (Figure 2b). Comparison of the air and helium flow data in Figure 3 provide some insight into possible explanations.

At a mass-flow rate of 5 L/min^{RTP}, the *additional* ΔP^2 (measured ΔP^2 minus predicted ΔP^2 for the fiber bundle) for helium is about 58% of the additional ΔP^2 for air (Figure 3). Since air and helium have comparable viscosities, but ten-fold different densities, this comparison suggests that roughly half of the additional ΔP^2 for air involves inertially-related pressure losses. At 5 L/min^{RTP} the dynamic gas head ($1/2\ \rho\bar{V}^2$) within the fibers is appreciably less than 0.1 mm Hg for air, and so inertial pressure losses within the fibers is not likely important. The largest estimated dynamic head along the entire IMO gas flow pathway appears to be in the gas feed tube/port opening (A = 0.03 cm^2) into the feed manifold (Figure 1b) for the fibers, and is roughly 10 mm Hg for air at 5 L/min^{RTP}, or nearly ten times less than the apparent inertially-related additional pressure drop. Thus, inertial effects associated with flow into and within this feed manifold may be playing some role, but a significant inertially related component still appears to be unaccounted for.

Roughly one-half of the additional pressure drop appears to be density independent, which suggests additional viscous dissipation not accounted for by compressible Poiseuille flow within the assumed fiber bundle. Several possible explanations require further study. The plotting of the fibers into the manifolds may be constricting the entrances and exits of the hollow fibers. The potting process itself may even be occluding some population of the fibers within the bundle. These are clearly important design and fabrication issues demanding further study, and an IMO prototype is being fabricated with several additional pressure taps (such as in the feed and exhaust manifolds) for partitioning the overall measured pressure drop along key points within the gas pathway. The compressible Poiseuille flow paradigm for hollow fibers, as validated in this study, will be an essential tool in the analysis and interpretation of these experiments.

Conclusions

The principal finding of this study is that the pressure-flow behavior measured in hollow fibers follows *compressible* Poiseuille flow theory, which predicts a linear relation between mass-flow rate and the difference in pressure *squared* across the fiber length. Incompressible Poiseuille flow theory predicts the pressure-flow behavior in hollow fibers satisfactorily up to about 100 mm Hg vacuum, whereas the applicability of compressible Poiseuille flow theory was established over the broad range of gas-phase pressure drops (up to −400 mm Hg) pertinent to intravenous and other forms of intracorporeal oxygenation. Demonstration that the pressure-flow behavior in hollow fibers follows compressible Poiseuille flow theory was essential to the interpretation of the measured pressure-flow behavior in our IMO. The IMO gas pathway engenders a signficantly greater pressure drop than attributable to compressible Poiseuille flow in its hollow fiber bundle. Compressible Poiseuille flow theory will be a valuable tool in further experimental studies of the pressure flow behavior within the IMO device.

Acknowledgment

This work was supported by the U.S. Army Medical Research, Development, Acquisition, and Logistics Command under contract No. DAMD17-94-C-4052. The views, opinions, and/or findings contained in this report are those of the authors and should not be construed as an official Dept. of the Army position, policy, or decision unless so designated by other documentation. The generous support of Medtronic Inc. and the McGowan foundation are also appreciated. Special thanks to Mr. Frank Walters for ongoing fabrication of IMO prototypes and test fiber banks.

Notation

d = hollow-fiber internal diameter
Le = fiber entrance length
$\mathfrak{R}$ = (species-dependent) gas constant
$\bar{V}$ = cross-sectional average fluid velocity
z = axial cylindrical coordinate

Subscripts/superscripts

atm = atmospheric pressure
o = evaluated at upstream end of fiber
l = evaluated at downstream end of fiber

Literature Cited

Fazzalari, F. L., R. H. Bartlett, M. R. Bonnell, and J. P. Montoya, "An Intrapleural Lung Prosthesis: Rationale, Design and Testing," *Artif. Orgs.*, **18**(11), 801 (1994).

Gerhart, P. M., R. J. Gross, and J. I. Hochstein, *Fundamentals of Fluid Mechanics*, Addison-Wesley, Reading, MA, p. 468 (1992).

Hattler, B. G., P. C. Johnson, P. J. Sawzik, F. D. Shaffer, M. Klain, L. W. Lund, G. D. Reeder, F. R. Walters, J. S. Goode, and H. S. Borovetz, "Respiratory Dialysis: A New Concept in Pulmonary Support," *ASAIO Trans.*, **38**, M322 (1992).

High, K. M., M. T. Snider, and G. Bashien, "Principles of Oxygenator Function: Gas Exchange, Heat Transfer, and Blood Artificial Surface Interaction," *Cardiopulmonary Bypass: Principles and Practice*, G. P. Gravlee, R. F. Davis, J. R. Utley, eds., Williams and Wilkins, Baltimore, p. 28 (1993).

Kyle, B. G., *Chemical and Process Thermodynamics*, Prentice-Hall, Englewood Cliffs, NJ (1984).

Mortensen, J. D., and G. Berry, "Conceptual and Design Features of a Practical, Clinically Effective Intravenous Mechanical Blood Oxygen/Carbon Dioxide Exchange Device," *Int. J. Artif. Orgs.*, **12**(6), 384 (1989).

Qi, Z., and E. L. Cussler, "Microporous Hollow Fibers for Gas Absorption I: Mass Transfer in the Liquid," *J. Memb. Sci.*, **23**, 321 (1985a).

Qi, Z., and E. L. Cussler, "Microporous Hollow Fibers for Gas Absorption II: Mass Transfer Across the Membrane," *J. Memb. Sci.*, **23**, 333 (1985b).

Shapiro, A. H., *The Dynamics and Thermodynamics of Compressible Fluid Flow*, Vol. I, Wiley, New York, p. 189 (1953).

Shelekhin, A. B., A. G. Dixon, and Y. H. Ma, "Adsorption, Permeation, and Diffusion of Gases in Microporous Membranes. II. Permeation of Gases in Microporous Glass Membranes," *J. Memb. Sci.*, **75**, 233 (1992).

Manuscript received July 24, 1995, and revision received Oct. 20, 1995.